Electronic supplementary information

Towards Sustainable Electrochemical Energy Storage:

Potassium-Based Dual-Graphite Batteries

Kolja Beltrop[a], Stephan Beuker[a], Andreas Heckmann[a], Martin Winter[a,b], Tobias Placke[a]

[a]University of Münster, MEET Battery Research Center, Corrensstr. 46, 48149 Münster, Germany
[b]Helmholtz Institute Münster, IEK-12, Forschungszentrum Jülich, Corrensstr. 46, 48149 Münster, Germany

Experimental

Electrode and electrolyte preparation

Electrode tapes for the negative and positive electrode consist of 90 wt.% KS6L graphite (Imerys Graphite & Carbon), 5 wt.% of conductive carbon black agent C-nergy™ Super C65 (Imerys Graphite & Carbon) and 5 wt.% of sodium carboxymethylcellulose (Na-CMC) as binder (Walocel CRT 2000 PPA 12, Dow Wolff Cellulosics). **Table S1** summarizes specific characteristics of the flake-type synthetic KS6L graphite.[1] The calculation of the interlayer distance and the crystallite height (L_c) was performed according to Iwashita et al.[2]

Table S1: D90 value of the particle size distribution, BET surface area, DFT surface area, basal plane surface area, "non-basal plane surface" area, ratio of basal to "non-basal plane surface" area, interlayer distance and L_c – crystallite height of the investigated KS6L-type graphite.[1]

Graphite	D90 / µm	BET surface area / $m_2 g_{-1}$	DFT surface area / $m_2 g_{-1}$	Basal plane surface area / $m_2 g_{-1}$	"Non-basal plane" surface area / $m_2 g_{-1}$	Ratio of basal to "non-basal plane" surface area / %	Interlayer distance / nm	L_c – crystallite height / nm
KS6L	8.5	19.04	20.52	11.25	9.27	55 : 45	0.335	114.833

The preparation process of the electrodes was performed as reported in our previous publication.[3] The average mass loading of the electrodes was 2.0±0.1mg cm^{-2}.

For the preparation of the different electrolyte solutions the following reagents and materials were used: *N*-butyl-*N*-methylpyrrolidinium bis(trifluorosulfonyl) imide (Pyr$_{14}$TFSI; Solvionic; purity: 99.9%), lithium bis(trifluorosulfonyl) imide (KTFSI; Solvionic; purity: 99.5%), ethylene sulfite (ES; Sigma Aldrich; 98%) were purchased and used as received.

An electrolyte mixture of Pyr$_{14}$FSI with 0.3 M of the conductive and electroactive potassium salt KTFSI and 2 wt.% ethylene sulfite was used as baseline electrolyte. The electrolyte preparation and storage as well as the cell manufacturing were carried out in an argon filled glove box (H$_2$O and O$_2$ < 0.1 ppm). Prior to use, the IL was dried, applying an ultra-

high vacuum procedure (< 1·10^{-2} Pa). The water content of the IL was less than 10 ppm, as determined by Karl Fischer titration.

Cell preparation and electrochemical characterization

All electrochemical measurements were conducted in lab-scale Swagelok type T-cells with a three-electrode set-up, as described in previous publications.[4, 5] For both, the negative and the reference electrodes, high-purity metallic potassium (K metal; Sigma Aldrich; purity: 99.95%) were applied. A glass microfiber filter (Whatman; grade GF/D) soaked with 120 μL of the corresponding electrolyte was used as separator. To ensure a sufficient wetting of the graphite electrodes by the viscous IL-based electrolyte, the assembled cells were equilibrated for 24 hours at room temperature (20 °C) before electrochemical characterization. Constant current charge/discharge cycling was performed on a Maccor 4000 battery test system within climatic chambers set to 20 °C.

Three different cell set-ups have been evaluated electrochemically: *(1)* Potassium intercalation/de-intercalation into a graphite-based anode (K vs. graphite; **Fig. 1 and Fig. S1**, see manuscript), *(2)* anion intercalation/de-intercalation into a graphite-based cathode (K vs. graphite; **Fig. 2**, see manuscript) and *(3)* potassium and anion intercalation/de-intercalation into a graphite-based anode and cathode, respectively (graphite vs. graphite, **Fig. 3 and Fig. S2**, see manuscript). For all charge/discharge investigations, a constant current rate of 10 mA g^{-1} for three formation cycles and 50 mA g^{-1} for the ongoing cycles was applied for both charge and discharge steps, which corresponds to a rate of 1C assuming a theoretical capacity of 50 mAh g^{-1} (determined from the active mass of the positive graphite electrode).

(1) The constant current cycling of KS6L-based graphite anodes in a half-cell set-up (K metal vs. graphite) was conducted with a specific current of 10 mA g^{-1} for three formation cycles and 50 mA g^{-1} for the ongoing cycles between 0.05 V and 1.5 V vs. K/K$^+$.

(2) The charge/discharge cycling of KS6L graphite cathodes in a half-cell set-up (K metal vs. graphite) was performed with a constant current of 10 mA g^{-1} for three formation cycles and 50 mA g^{-1} for the ongoing cycles between 3.4 V and 5.0 V vs. K/K$^+$.

(3) The constant current cycling of the potassium-based dual-graphite (K-DGB) cells was carried out with a constant charge and discharge current of 10 mA g^{-1} for the first three cycles in order to provide a homogeneous SEI-formation, while from the 4th cycle the current is increased to 50 mA g^{-1}. In this set-up, the graphite cathode potential during charge/discharge of the cell is controlled via the reference electrode (3.4 V and 5.0 V vs. K/K$^+$) which results in a variable cell voltage and anode potential. The anode/cathode capacity balancing is not optimized in this system (anode is largely oversized) and needs to be further improved in future studies to optimize the energy density of the cell. The capacity of the dual-

graphite system is calculated with respect to the cathode capacity (related to the mass of the graphite cathode).

Comments to anode potential profiles in dual-graphite cell (Fig. 3A)

From Figure 3A in the manuscript it is clearly visible, that the anode potential profile and, thus, the potassium storage mechanism into/on graphite changes during charge/discharge cycling. In the K-DGB presented in this work, a largely oversized anode is used to study the principle working mechanism of the system and to provide the evidence of feasibility of the K-DGB. Structural changes of graphite during cycling could cause an increased capacitive charge, which, in turn, can compensate the cathode capacity. Thus, potassium adsorption rather than potassium intercalation may become the predominantly potassium storage mechanism and will have a severe impact of the electrochemical operating window of the negative electrode (shifted to higher potentials). By systematically balancing anode and cathode according to their practical capacities, these effects can be diminished, as indicated by the potential profile of the anode half-cell in Figure 1c. Therefore, it is highly probable, that potassium intercalation becomes the main storage mechanism again. According to the voltage profiles of half and full-cells, we do not expect graphite exfoliation as the main origin for the change in the potential profile. However, Raman and additional XRD measurements of cycled electrodes have to be conducted, in order to fully exclude possible exfoliation of the graphite structure. Furthermore, additional electrochemical measurements are needed to gain a deeper understanding of the working mechanism of the invented K-DGB.

Further electrochemical results

In addition to the discussion in the manuscript and in order to gain a deeper understanding on the potassiation/depotassiation into graphite, differential capacity (dQ/dV) profiles for selected cycles are depicted in **Fig. S1**.

The effect of the addition of ethylene sulfite (ES) to the baseline electrolyte is discussed in the following sequence in more detail. In the lithium-based dual-graphite cell, applying $Pyr_{14}TFSI$ as electrolyte solvent, a severe co-intercalation of Pyr_{14}^+ cations into the graphitic anode is observed during the lithiation process. This process is accompanied by severe exfoliation of the graphite structure, thus, deteriorating the overall cell performance and resulting in rapid capacity fading.[6-8] By addition of suitable electrolyte additives, such as ES, we could show in a previous publication that the lithiation/de-lithiation process in the lithium-based dual-graphite cell can be highly reversible.[6]
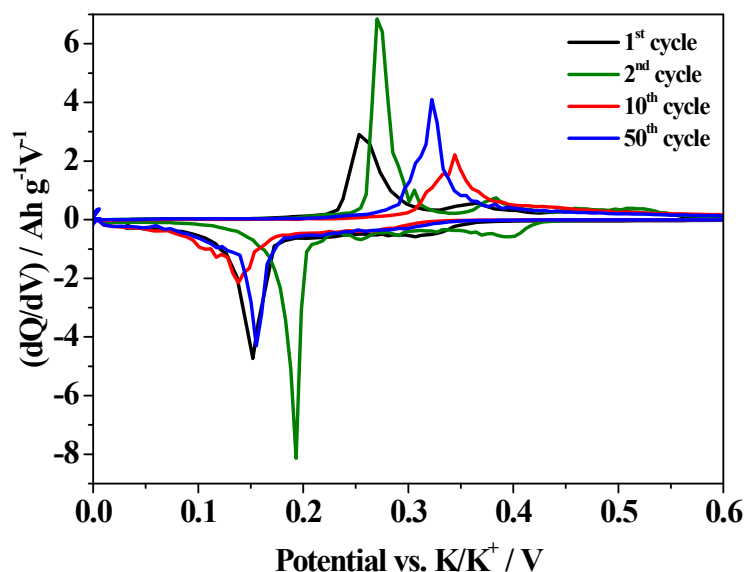
Fig. S1: Differential capacity (dQ/dV) profiles for selected cycles taken from the constant current cycling of KS6L graphite / K metal cells in a potential range between 0.05 V and 1.5 V vs. K/K+. Electrolyte: Pyr$_{14}$TFSI, 0.3 M KTFSI + 2 wt.% ES. Charge/discharge current: 10 mA g^{-1} (cycle 1 and 2) and 50 mA g^{-1} (cycle 10 and 50).

A possible incompatibility of the graphite anode and the ionic liquid electrolyte was also assumed to take place in the corresponding potassium-based dual-graphite system and, therefore, ES as effective SEI additive was used to prevent the graphite anode from ongoing exfoliation. Interestingly, constant current cycling investigations applying the baseline electrolyte without ES as SEI forming additive shows, that, contrary to expectations, a stable cycling performance with greatly reduced solvent co-intercalation compared to the lithium system could be achieved (**Fig. S2**).
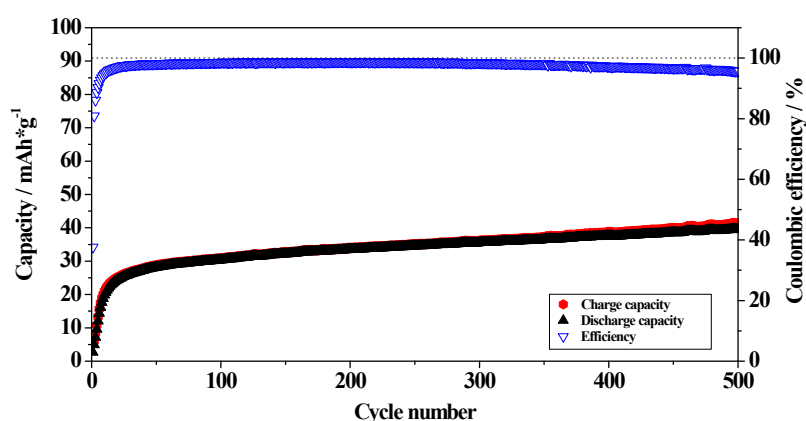
Fig. S2: Constant current cycling of graphite (cathode) / graphite (anode) cells for selected cycles between 3.4 V and 5.0 V vs. K/K+ at a charge/discharge current of 50 mA g^{-1} applying the baseline electrolyte (Pyr$_{14}$TFSI, 0.3 M KTFSI) without ES as electrolyte additive.

The higher potential of potassium intercalation into graphite compared to the lithium system is most likely a possible reason for the reduced solvent co-intercalation. However, the reduced discharge capacity compared to the system with ES indicates a beneficial effect of ES on the overall cell performance as also stated by Rothermel et al.[6] Additional electrochemical investigations are needed to further evaluate the mechanism of solvent co-intercalation into graphite in the specific systems and the beneficial influence of ES on the discharge capacity.

References
1. T. Placke, O. Fromm, S. Rothermel, G. Schmuelling, P. Meister, H. W. Meyer, S. Passerini and M. Winter, *ECS Transactions*, 2013, **50**, 59-68.
2. N. Iwashita, C. R. Park, H. Fujimoto, M. Shiraishi and M. Inagaki, *Carbon*, 2004, **42**, 701-714.
3. T. Placke, S. Rothermel, O. Fromm, P. Meister, S. F. Lux, J. Huesker, H. W. Meyer and M. Winter, *Journal of the Electrochemical Society*, 2013, **160**, A1979-A1991.
4. T. Placke, O. Fromm, S. F. Lux, P. Bieker, S. Rothermel, H. W. Meyer, S. Passerini and M. Winter, *Journal of the Electrochemical Society*, 2012, **159**, A1755-A1765.
5. T. Placke, P. Bieker, S. F. Lux, O. Fromm, H. W. Meyer, S. Passerini and M. Winter, *Zeitschrift für Physikalische Chemie*, 2012, **226**, 391-407.
6. S. Rothermel, P. Meister, G. Schmuelling, O. Fromm, H. W. Meyer, S. Nowak, M. Winter and T. Placke, *Energy & Environmental Science*, 2014, **7**, 3412-3423.
7. M. Nadhérna, J. Reiter, J. Moskon and R. Dominko, *Journal of Power Sources*, 2011, **196**, 7700-7706.
8. S. F. Lux, M. Schmuck, G. B. Appetecchi, S. Passerini, M. Winter and A. Balducci, *Journal of Power Sources*, 2009, **192**, 606-611.